Quantification of lateral repulsion between coadsorbed CO and N on Rh(100) using temperature-programmed desorption, low-energy electron diffraction, and Monte Carlo simulations

Quantification of lateral repulsion between coadsorbed CO and N on Rh(100) using temperature-programmed desorption, low-energy electron diffraction, and Monte Carlo simulations

A. P. van Bavel, M. J. P. Hopstaken, D. Curulla, and J. W. Niemantsverdriet[a)]
Eindhoven University of Technology, Schuit Institute of Catalysis, P. O. Box 513, 5600 MB Eindhoven, The Netherlands

J. J. Lukkien and P. A. J. Hilbers[b)]
Eindhoven University of Technology, Department of Mathematics and Computer Science, P.O. Box 513, 5600 MB Eindhoven, The Netherlands

(Received 10 February 2003; accepted 2 April 2003)

Temperature programmed desorption of CO coadsorbed with atomic N on Rh(100), reveals both long- and short-range interactions between adsorbed CO and N. For CO desorption from Rh(100) at low coverage we find an activation energy E_a of 137 ± 2 kJ/mol and a preexponential factor of $10^{13.8\pm0.2}$ s^{-1}. Coadsorption with N partially blocks CO adsorption and destabilizes CO by lowering E_a for CO desorption. Destabilization at low N coverage is explained by long-range electronic modification of the Rh(100) surface. At high N and CO coverage, we find evidence for a short-range repulsive lateral interaction between CO_{ads} and N_{ads} in neighboring positions. We derive a pairwise repulsive interaction $\omega^{NN}_{CO-N}=19$ kJ/mol for CO coadsorbed to a $c(2\times2)$ arrangement of N atoms. This has important implications for the lateral distribution of coadsorbed CO and N at different adsorbate coverages. Regarding the different lateral interactions and mobility of adsorbates, we propose a structural model which satisfactorily explains the observed effects of atomic N on the desorption of CO. Dynamic Monte Carlo simulations were used to verify the experimentally obtained value for the CO–N interaction, by using the kinetic parameters and interaction energy derived from the temperature-programmed desorption experiments. © *2003 American Institute of Physics.* [DOI: 10.1063/1.1577536]

I. INTRODUCTION

Lateral interactions between adsorbates are crucially important in catalytic surface reactions, as they greatly influence reactivity at higher coverage—for instance, in the decomposition of NO on different transition metals.[1,2] Therefore, quantitative information about lateral interactions is essential to model reaction kinetics correctly at high coverages, as met under realistic catalytic conditions. Obviously, single-crystal adsorption calorimetry (SCAC) is the most direct way to determine lateral interactions in a quantitative fashion.[1] Lateral interactions can also be derived from temperature programmed experiments, such as temperature-programmed desorption (TPD) or temperature-programmed secondary ion mass spectrometry (TPSIMS), by studying the coverage dependence of reaction kinetics.

Lateral interactions are often accounted for by assuming a linear dependence between the kinetic parameters and global coverage in the so-called mean-field approach. However, this approach generally overestimates the effect of lateral interactions at low coverages, particularly if interactions are repulsive. A more rigorous description of lateral interactions takes the individual arrangement of adsorbates into account. In order to include these in the kinetics, pairwise interaction energies need to be estimated or determined experimentally.

Monte Carlo simulations provide a way to specify the local environment of a reacting molecule.[3,4] This allows for modeling of lateral interactions, local reconstructions, and diffusion of adsorbates. Our interest is to describe the kinetics of surface reactions on highly covered surfaces by including lateral interactions on a local basis. We focus on the system CO+NO on Rh(100), which is of interest for automotive exhaust catalysis[5,6] and for which a number of elementary kinetic parameters have recently been obtained.[2,7,8] The reason for selecting Rh(100) instead of (111) is that the chemistry on the latter may be dominated by defects, whereas reactions on Rh(100) are expected to reflect intrinsic chemistry of the (100) surface, as was observed for the elementary reaction CO+O to CO_2.[8]

To the best of our knowledge, there is hardly any quantitative information available on interactions between CO and coadsorbates on rhodium.

Daniel and White[9] studied the desorption of CO from N-precovered Rh(100). Presence of coadsorbed N atoms lowered both the CO desorption temperature and CO uptake, and gave rise to a new low-temperature CO desorption state. However, the authors studied only a limited range of coverages and gave no quantitative information on the N–CO interaction. Other studies addressing the influence of an atomic coadsorbate on the binding of CO on rhodium surfaces are

a)Author to whom correspondence should be addressed.
Fax: +0031 40 247 3481. Electronic mail: J.W.Niemantsverdriet@tue.nl
b)Currently at Eindhoven University of Technology, Department of Biomedical Engineering, P. O. Box 513, 5600 MB Eindhoven, The Netherlands.

mainly concerned with the effect of electropositive elements such as sodium or potassium. These promoters generally stabilize bonding of CO by increasing backdonation to the CO $2\pi^*$ molecular orbital.[10,11] On the contrary, coadsorption of CO with electronegative elements such as sulphur[12] or iodine[13] leads to destabilization of CO.

The purpose of this paper is to quantify the lateral repulsion energy between coadsorbed CO and atomic nitrogen on Rh(100). The strategy is to find ordered structures in which the numbers of neighbors of the CO molecule can be estimated, determine the adsorption energy of CO in this arrangement, and derive the lateral repulsion energy. As CO occupies different adsorption sites with and without coadsorbed N atoms, density-functional calculations are needed to analyze differences in the heat of adsorption of CO on different sites. Finally the thus-determined lateral interaction energy will be tested in a dynamic Monte Carlo simulation of CO desorption in the presence of N atoms, hence simulating a TPD experiment for direct comparison.

II. EXPERIMENTAL METHODS

A. TPD and LEED measurements

The experiments were done in a stainless-steel ultrahigh-vacuum (UHV) apparatus with a base pressure of 2×10^{-11} mbar, previously described in Ref. 2. The rhodium crystal of (100) orientation has a thickness of about 1.2 mm and was mounted on a moveable sample rod by two tantalum wires of 0.3 mm diameter, pressed into small grooves on the side of the crystal. This construction allows for resistively heating the sample up to 1450 K. The sample can be cooled by a flow of liquid nitrogen to 100 K. Temperature was measured with a Chromel–Alumel thermocouple spotwelded to the back of the crystal. The crystal surface was cleaned as described previously.[2] Low-energy electron diffraction (LEED) experiments were performed with a reverse-view, four-grid Auger electron spectroscopy (AES)/LEED optics (Spectaleed, Omicron Vakuumphysik GmbH). LEED data were obtained with an electron beam current between 20 and 30 μA.

Nitric oxide (Hoek Loos, 99.5% pure) and carbon monoxide (Hoek Loos, 99.997% pure) were used without further purification. Temperature programmed experiments were done with a heating rate of 5 K/s. Calibration of the CO coverage was done by setting the saturation coverage at 300 K at 0.75 monolayer (ML), according to de Jong *et al.*[14] The N coverage is determined as described in Ref. 2.

B. Theoretical details

We have performed a series of calculations to determine the adsorption energy of CO at different sites (on-top and fourfold hollow site) on Rh(100). We have used the Vienna *ab initio* simulation program VASP. We have modeled the Rh(100) surface by means of a three-layer slab representing a $p(4\times4)$ unit cell and six vacuum layers. The relative positions of the atoms are those as in the bulk, with an optimized lattice parameter of 3.850 Å. Relaxation of the first layer has been allowed in all calculations. The electron–ion interaction is described by optimized ultrasoft pseudopotentials for C, O, and Rh with a cutoff energy of 300 eV. Nonlocal corrections to the exchange-correlation functional in the form of the generalized gradient approximation proposed by Perdew *et al.* have been used. Brillouin-zone integration has been performed using grids of $(4\times4\times1)$ **k** points.

The thermal desorption data have been simulated with a dynamic Monte Carlo method in which the Rh(100) surface is modeled by a square 128×128 grid with periodic boundary conditions as described in detail by Jansen.[3] Rate constants for the reactions without lateral interactions are given as Arrhenius expressions $k=\nu\exp(-E_a/RT)$. Lateral interactions are modeled by letting the effective activation energy depend on the neighborhood of the reacting particles. As we limit ourselves to desorption, the activation energy is written in the form

$$E_{\text{eff}}=E_a-\Sigma_i n_i\omega_i^{\text{NN}}, \tag{1}$$

in which E_a is the activation energy at zero coverage, n_i is the number of nearest-neighboring i particles, and ω_i^{NN} is the nearest neighbor (NN) pairwise lateral interaction term. The preexponential factor is assumed to be constant with coverage. The simulations were carried out using the computer program CARLOS,[4] which is a general purpose program that admits specification of the adlayer, the species, and the microscopic steps as input.

III. RESULTS

A. Desorption of CO from Rh(100)

TPD spectra (heating rate $\beta=5$ K/s), obtained after dosing various amounts of CO on Rh(100) below 200 K, are shown in Fig. 1. Coverages of CO are expressed as monolayers (adsorbate/metal substrate surface atom). The general shape and peak positions of the spectra agree with those reported previously by de Jong *et al.*[14] Also the CO uptake curve (not shown) is similar to the uptake curve presented in the former study and is best described by the precursor model by Kisliuk,[15] indicating that CO adsorbs via a mobile precursor state.[14]

At low coverage ($\theta_{\text{CO}}<0.10$ ML), CO desorbs with a maximum rate around 500 K which is 10 K higher than measured by de Jong *et al.*[14] This can be explained by the lower heating rate ($\beta=3.5$ K/s) applied in the former study. Upon increasing the coverage up to 0.50 ML, CO desorbs in a single state, shifting slightly to lower temperatures by 25 K. This is in line with the nearly constant heat of adsorption for CO on Rh(100) in this coverage range, as determined by Kose *et al.*[16] using microcalorimetry and by Medvedev *et al.*[17] using reverse flash measurements, respectively. Up to $\theta_{\text{CO}}=0.50$ ML, only on-top sites are populated. Because repulsion between CO molecules in next-nearest-neighboring (NNN) sites is only small,[16] this results in the formation of a $c(2\times2)$ structure CO on Rh(100),[14,18,19] which we observed as well in LEED (not shown).

Above $\theta_{\text{CO}}>0.50$ ML, a poorly resolved shoulder grows in around 400 K. This shoulder is due to compression of the CO overlayer, with CO increasingly populating bridge positions and simultaneously depopulating the on-top sites, as indicated by vibrational spectroscopy[14,18] and high-resolution

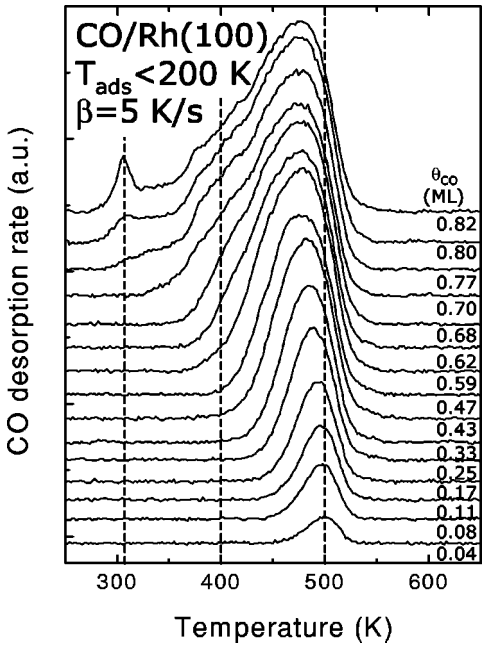

FIG. 1. CO TPD spectra for various amounts of CO adsorbed below 200 K on Rh(100). The applied heating rate is 5 K/s.

photoelectron spectroscopy.[19] The appearance of this new desorption state is accompanied by a steep decrease in both sticking coefficient and heat of adsorption.[16]

For CO coverages exceeding 0.75 ML, an additional desorption channel appears around 305 K. This is due to further compression of the $p(4\sqrt{2}\times\sqrt{2})R45°$ structure which forms at $\theta_{CO}=0.75$ ML into a $c(2\times6)$ structure with $\theta_{CO}=0.83$ ML.[14] This was not observed in the TPD spectra reported by de Jong *et al.*, because CO was adsorbed at higher temperature. However, this state could be populated at 270 K by dosing CO with $p_{CO}=1\times10^{-6}$ mbar. A similar desorption state was also reported by Baraldi *et al.*,[20] after a CO saturation dose at 150 K. Probably, the residence time of a physisorbed CO molecule is too short around room temperature for accommodation of additional CO molecules within the $p(4\sqrt{2}\times\sqrt{2})R$ 45° structure in a chemisorbed state.

Application of Chan–Aris–Weinberg ($CAW_{\frac{1}{2}}$) analysis[21] to the spectra in Fig. 1 yields an activation barrier of $E_a=137\pm2$ kJ/mol and a preexponential factor $\nu=10^{13.8\pm0.2}$ s^{-1} in the limit of zero CO coverage. These values are verified by the Redhead equation[22] ($T_{max}=502$ K, $\beta=5$ K/s, $\nu=10^{13.8}$ s^{-1} from $CAW_{\frac{1}{2}}$ analysis), which yields $E_a=137$ kJ/mol.

Coverage-corrected leading-edge analysis[7] allows for the determination of kinetic parameters for CO desorption as a function of initial coverage. At low CO coverage we find $E_a=140\pm3$ kJ/mol and $\upsilon=10^{14.1\pm0.3}$ s^{-1}, in good agreement with $CAW_{\frac{1}{2}}$ analysis. Upon increasing the CO coverage up to, E_a continuously decreases weakly to ca. 110 kJ/mol at $\theta_{CO}=0.50$ ML. These results are in good agreement with the nearly constant heat of adsorption in this coverage range as determined with calorimetry.[16,17]

Close to saturation, we observe a new well-resolved desorption state around 305 K, associated with the compression of the $p(4\sqrt{2}\times\sqrt{2})R45°$ into a $c(6\times2)$-CO/Rh(100) structure. Redhead analysis ($T_{max}=305$ K, $\beta=5$ K/s; assuming $\nu=10^{13\pm1}$ s^{-1}) yields $E_a=78\pm6$ kJ/mol. This is in good agreement with the differential heat of adsorption of 80 kJ/mole for CO adsorption at 300 K close to the CO saturation coverage.[16]

DFT calculations for CO on a Rh(100) slab yield adsorption energies of 178 kJ/mol for CO in both on top and fourfold hollow sites.

B. Effect of N atoms on CO desorption from Rh(100)

To study the interaction between these adsorbates, we have coadsorbed atomic N and CO. We exclude the formation of isocyanate (NCO) on rhodium, as it has been shown by Kiss and Solymosi[23] that NCO readily decomposes to CO and N on Rh(111) even at 150 K, while coadsorbed oxygen has a slightly stabilizing effect.[24] Kostov *et al.* studied the formation of NCO from CO, coadsorbed with partly dissociated NO on Ru(0001).[25] In the absence of coadsorbed O, formation of NCO was not observed.[26]

Overlayers of atomic N were prepared by dissociative adsorption of NO at 400 K, followed by selective removal of O at 400 K under an ambient CO pressure ($p_{CO}=2\times10^{-8}$ mbar, $t=180$ s). Importantly, O_{ads} is completely removed in this fashion, while the residual amount of CO_{ads} desorbs by shortly annealing to 600 K. The procedure allows the preparation of N overlayers on Rh(100) up to around $\theta_N=0.3$ ML without detectable contamination.

Figure 2 shows CO TPD spectra for CO adsorbed on N-precovered Rh(100) with $\theta_N=0.14$ ML and $\theta_N=0.27$ ML. At the lower nitrogen coverage ($\theta_N=0.14$ ML, left panel) up to $\theta_{CO}\approx0.30$ ML CO desorbs in a single state around 480 K. This is slightly lower than in the absence of N_{ads}, where CO initially desorbs around 500 K. $CAW_{\frac{1}{2}}$ analysis yields an activation energy $E_a=133\pm3$ kJ/mol and a preexponential factor $\nu=10^{13.9\pm0.2}$ s^{-1} in the limit of zero CO coverage and $\theta_N=0.14$ ML.

At $\theta_{CO}\approx0.35$ ML, a poorly resolved shoulder develops around 400 K, in the same temperature range for the case when CO is the only adsorbate (Fig. 1). Upon further increasing θ_{CO} to 0.44 ML, a new CO desorption feature appears around 350 K. Finally, a new desorption state is observed around 250 K when θ_{CO} is close to saturation. This is in reasonable agreement with the low-temperature CO desorption features observed by Daniel and White[9] at comparable coverages.

At intermediate N coverage ($\theta_N=0.27$ ML, right panel, Fig. 2), the first CO molecules desorb at an progressively lower temperature of 465 K. $CAW_{\frac{1}{2}}$ analysis yields $E_a=122\pm2$ kJ/mol and $\nu=10^{13.4\pm0.2}$ s^{-1} in the limit of zero CO coverage. Upon increasing θ_{CO}, the same qualitative features are observed as for the lower N coverage. However, the 400 K shoulder associated with CO–CO repulsion can hardly be distinguished. On the other hand, the CO desorption features around 350 and 250 K become clearly more pronounced. Since this is not observed in the absence of N_{ads} and these desorption states become more distinct with increasing N coverage, we assign these features to direct repulsion between atomic N and CO.

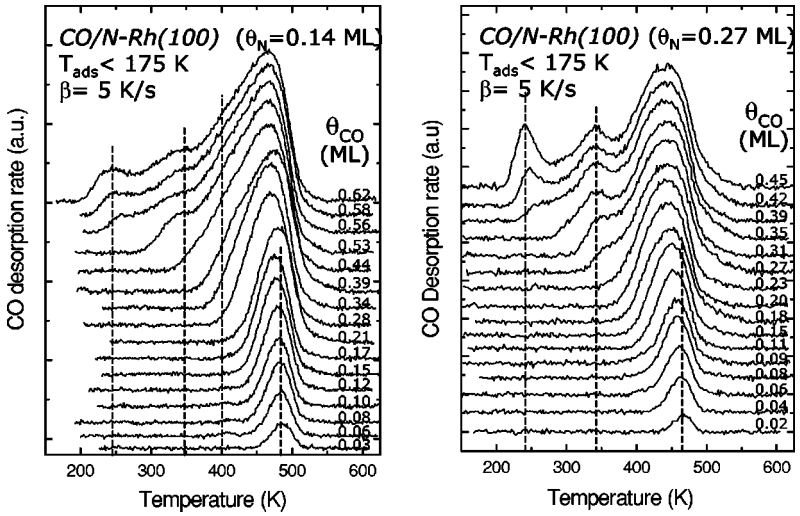

FIG. 2. CO TPD spectra for various amounts of CO adsorbed below 200 K on N-precovered Rh(100) with $\theta_N=0.14$ ML (left panel) and $\theta_N=0.28$ ML (right panel). Fixed amounts of atomic N were deposited by dissociative adsorption of NO and subsequent removal of O by stripping of with CO. The applied heating rate is 5 K/s.

It is, however, not possible to extract a value for the CO–N pairwise interaction from these experiments. As the mixed CO+N adlayer is undefined in terms of ordering or island formation and diffusion of a molecular adsorbate like CO is fast,[27] many configurations of desorbing CO molecules with different numbers of neighboring N atoms are possible.

To circumvent this problem, we have examined the desorption of CO from an ordered $c(2\times2)$-N/Rh(100) structure.[28] Preparation of N_{ads} on Rh(100) by dissociative adsorption of NO and subsequent removal of O_{ads} as described above deposits around 0.3 ML of N_{ads} at maximum. Higher N coverages can be achieved by exposing the Rh(100) crystal to a mixture of CO and NO above the NO desorption temperature (400 K) and below the onset of N_2 formation (550 K). In this way, we can deposit up to around 0.5 ML N_{ads}, as a clear $c(2\times2)$ pattern can be seen by LEED (Fig. 3). We cannot conclude whether all N atoms are part of the $c(2\times2)$ structure and whether all N atoms reside on the surface or that a fraction diffuses into subsurface positions. Nevertheless, the prominent $c(2\times2)$ pattern in LEED indicates that considerable parts of the surface are covered by this ordered array of N atoms.

Figure 4 shows CO desorption spectra, saturated with $N_{ads}[c(2\times2)-N_a]$. At the lowest CO coverage, only broad and poorly resolved desorption features can be observed between 225 and 500 K. Upon increasing the CO coverage, a sharp and increasingly dominant CO desorption state arises at 240 K. We attribute this state to the adsorption of CO in the $c(2\times2)$ N–Rh(100) environment. Using the Redhead equation ($T_{max}=240$ K and 5 K/s, assuming $\nu=10^{13\pm1}$ s^{-1}) we find $E_a=60\pm10$ kJ/mol for CO desorbing out of the $c(2\times2)$-N arrangement. The weaker additional desorption states at higher temperatures are tentatively attributed to CO desorbing out of defects in the $c(2\times2)$-N structure.

The corresponding LEED pattern in Fig. 3 confirms that CO does not destroy the ordered N layer to an appreciable extent, since the $c(2\times2)$ pattern remains prominently visible after coadsorption of CO and heating to 600 K. Note that the LEED pattern provides no evidence for coadsorbate-induced reconstructions. The weakening of the pattern is attributed to imperfect ordering of the coadsorbed CO in the ordered N overlayer. Also we cannot exclude that the presence of coadsorbed CO promotes N atoms into subsurface sites.

CO uptake curves were constructed by plotting the CO coverage as a function of exposure on clean and N-precovered Rh(100) with different N coverages (not shown). From the initial slopes of the uptake curves at $\theta_{CO}=0$, it appears that the initial CO sticking coefficient is hardly influenced by the presence of N_{ads}. This is consistent with precursor-mediated adsorption kinetics: an incoming CO molecule initially gets trapped in a physisorbed state and will diffuse rapidly across the surface until it finds an empty adsorption site unaffected by N_{ads}. The effect of N atoms on the CO uptake becomes apparent at $\theta_{CO}<0.20$ ML, and the CO sticking probability becomes lower with increasing N coverage. Also, the CO saturation coverage decreases with increasing amounts of N_{ads} as part of the CO adsorption sites surface are blocked, in agreement with Daniel and White.[9] A similar effect has been observed for N/Rh(110) (Ref. 29) and for I/Rh(111) (Ref. 13).

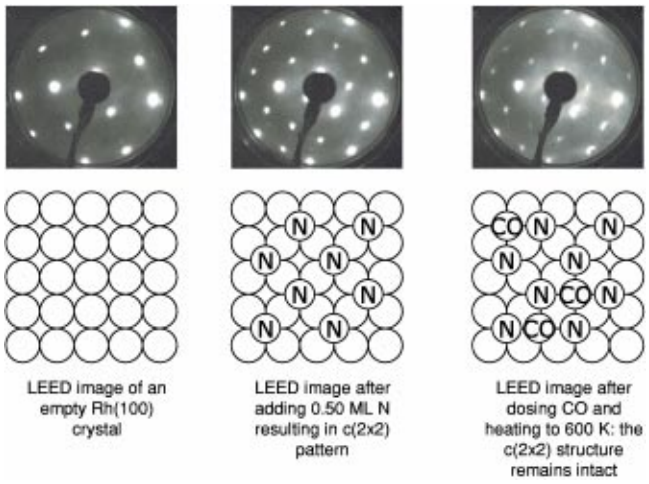

FIG. 3. LEED images of (left) a clean Rh(100) surface (middle) a $c(2\times2)$-N_{ads} /Rh(100) (right) CO adsorbed below 200 K on a $c(2\times2)$-N_{ads} /Rh(100) and heated up to 600 K. The electron energy was 145 eV.

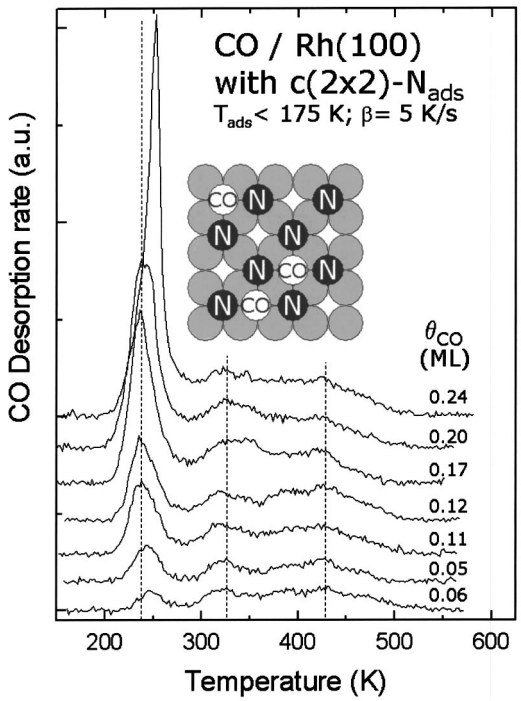

FIG. 4. CO TPD spectra for various amounts of CO adsorbed below 200 K on $c(2\times2)$-N_{ads} /Rh(100). Fixed amounts of atomic N were deposited by simultaneous dissociative adsorption of NO and removal of O by CO. The applied heating rate is 5 K/s.

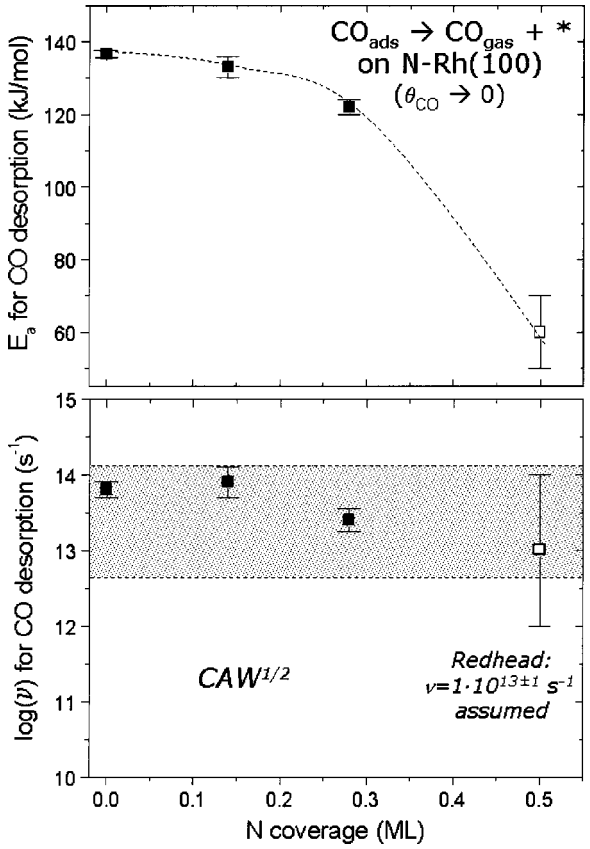

FIG. 5. Kinetic parameters for CO desorption [activation energy E_a (top) and preexponential factor ν (bottom)] as a function of N coverage. For the lower N_{ads} coverages (solid symbols) kinetic parameters were determined by $CAW\frac{1}{2}$ analysis ($\theta_{CO}\rightarrow 0$) and for the highest N coverage (open symbol) we have applied the Redhead equation to the 240 K desorption feature (Fig. 4), assuming $\nu=10^{13\pm1}$ s^{-1}. The dashed line through the data points for E_a has been drawn as a guide for the eye.

Figure 5 shows the kinetic parameters for CO desorption, i.e., activation energy E_a (upper panel) and preexponential factor ν (lower panel), as a function of the N-precoverage. Upon increasing θ_N from 0 to 0.27 ML, E_a only slightly decreases from 137 to 122 kJ/mol, while the preexponential factor is practically constant around $10^{13.7}$ s^{-1}. At 0.5 ML of N atoms, however, the CO molecules are less strongly bound with E_a about 60 kJ/mol. From this figure it immediately follows that the sudden decrease of the activation energy cannot be modeled by a simple mean-field approach (i.e., by numerical integration of the Polanyi–Wigner equation with a coverage dependence) as the decrease is not linear.

We use the latter value to estimate the repulsion between CO and nearest-N-neighbor atoms in the Discussion section.

IV. DISCUSSION

Before we address the interaction energy between CO and N, we first discuss a number of issues around the adsorption of CO on Rh(100).

A. Kinetics of CO desorption from Rh(100)

Kinetic parameters for CO desorption from Rh(100) as reported by various researchers are summarized in Table I. Our values for the kinetic parameters are generally in good agreement with those previously reported.[14,20,30,31] Note that the high value of the preexponential factor, reported earlier by our group,[14] is due to an error in application of the Chan–Aris–Weinberg equation for ν, where the authors divided by T_{max} instead of T_{max}^2 in the term before the exponent. Dividing the erroneous value of $10^{16.6}$ by the peak maximum temperature of 500 K yields a value of $10^{13.9}$ s^{-1}, similar to the value in the present work. Also the values reported by Wei *et al.*,[31] obtained by following the CO coverage using time resolved EELS under isothermal conditions with modulated beams of CO, appear to be too high.

Because molecular adsorption of CO on Rh surfaces is nonactivated, the activation energy for desorption equals the heat of adsorption. Indeed, microcalorimetry indicates a value of 118 kJ/mol for the differential heat of adsorption[16] and reverse flash indicates a bond energy of 121 kJ/mol ($\theta_{CO}\rightarrow 0$).[17] This enables us to construct a quantitative one-dimensional potential energy diagram for CO adsorption on Rh(100). However, the bond energy of 33 kJ/mol for the physisorbed state[17] would result in an unrealistically high barrier for adsorption of CO.

It remains unclear why theory fails to predict the correct adsorption energy for CO on Rh(100). Table II summarizes calculated values for the adsorption energies by different groups. DFT calculations by Eichler and Hafner[32] predict an adsorption energy of 215 kJ/mol for bridged CO ($\theta_{CO}=0.25$ ML). Recent calculations by Hammer *et al.*,[33] using a more sophisticated approach which corrects for overbinding more efficiently, predict an adsorption energy of 175 kJ/mol, also for CO in the bridge site ($\theta_{CO}=0.25$ ML). Our calcula-

TABLE I. Kinetic parameters for CO desorption from Rh(100) and heat of adsorption on Rh(100) in the limit of zero CO coverage.

Method	E_a (kJ/mol)	ν (s^{-1})	Reference
TPD (CAW$\frac{1}{2}$)	137±2	$10^{13.8\pm0.2}$	This work
TPD (leading edge)	140±3	$10^{14.1\pm0.3}$	This work
TPD (CAW$\frac{1}{2}$)	131±4	$10^{13.9\pm0.3}$ [a]	14
TPD (CAW$\frac{1}{2}$)	134	$10^{12.9}$	30
single beam	135±8	$10^{14.5\pm0.9}$	31
modulated beam	149±10	$10^{16.3\pm1.1}$	31
TPD	140	$10^{13.5}$	20
-	q_{ads} (kJ/mol)		-
SCAC	118		16
Reverse flash	121		17

[a]After correction for an incorrectly applied formula in Ref. 14.

tions predict an adsorption energy of 178 kJ/mol for both CO adsorbed in the top and the hollow site (with $\theta_{CO}=0.0625$ ML). These values are clearly too high, compared to the experimentally determined adsorption energy of 120–140 kJ/mol.[16,17] In addition, the bridge site is found to be energetically most stable, in contrast with all experimental observations.[14,19–21] Much better agreement between calculations and experiment is obtained for the CO bond energy on different Ni and Pd surfaces.[33] Clearly, the large discrepancies found for CO adsorption on Rh(100) require further theoretical investigation.

Lateral repulsion between mutual CO molecules only comes into play at higher coverage. Upon filling of the $c(2\times2)$-CO structure on Rh(100) structure ($\theta_{CO}\leqslant0.50$ ML), the heat of adsorption is almost constant[16,17] and CO desorbs in a single state. When θ_{CO} exceeds 0.50 ML, CO is compressed into a denser structure, as evidenced from the appearance of a shoulder in TPD. This is accompanied by reorganization of the CO overlayer, with increasing population of bridge sites and depopulation of top sites.[14,19–21] Also the sticking coefficient and the heat of adsorption sharply fall off around 0.50 ML CO coverage. Modeling the decrease in heat of adsorption using a Monte Carlo method, Kose *et al.*[16] derived a pairwise lateral repulsive energy of 9 kJ/mol for the CO–CO interaction (ω^{NN}_{CO-CO}).

B. Repulsive interactions between CO and N atoms

Figure 6 shows selected CO-TPD traces for two different N coverages.

At N coverages leaving sufficient space on the surface for CO to adsorb in sites not directly adjacent to N atoms, the desorption of CO shifts nevertheless to slightly lower temperatures, indicating that CO is somewhat destabilized ($\theta_N=0.14$ ML, both left and right panels). We attribute this effect to a slight modification of the electrostatic potential of Rh(100) covered by N atoms. Similar effects were reported for low amounts of CO desorbing from iodine-precovered Rh(111).[13] Also, DFT calculations indicate that coadsorption with sulphur slightly lowers the CO bond energy on Rh(111) for intermediate coverages ($\theta_S=\theta_{CO}=0.25$ ML).[12] Coadsorption of CO on N/Rh(110) has also been observed to shift desorption of both CO and N_2 to lower temperatures. In this case determination of kinetic parameters was complicated due to formation of separated phases and the existence of multiple reconstructions.[29]

The reason that CO desorption goes faster with increasing number of nitrogen (or sulphur; iodine) atoms at low CO coverage is probably that the electronegative atoms modify the electrostatic potential of the surface with a long-range effect that is similar but opposite in sign as small amounts of alkali do.[34] As a result the CO becomes destabilized on the entire surface, also when adsorbed further away from an adsorbed N atom.

At relatively high CO coverage (right panel), a small amount of N_{ads} already leads to significant compression of the CO domains, as a clear shoulder is present while for CO desorption from a clean Rh(100) surface this is first observed for $\theta_{CO}>0.50$ ML. This implies separated domains of N at-

TABLE II. Calculated adsorption energies for CO on Rh(100) in kJ/mol.

		Coverage (ML)				
Group	Site	1/16	1/4	2/4	3/4	4/4
Eichler and Hafner[a]	Top		191	188	150	191
	Bridged		215	202	176	215
	Hollow		207	189	151	207
Hammer *et al.*[b]	Bridged		175			
This work	Top	178				
	Hollow	178				

[a]Reference 32.
[b]Reference 33.

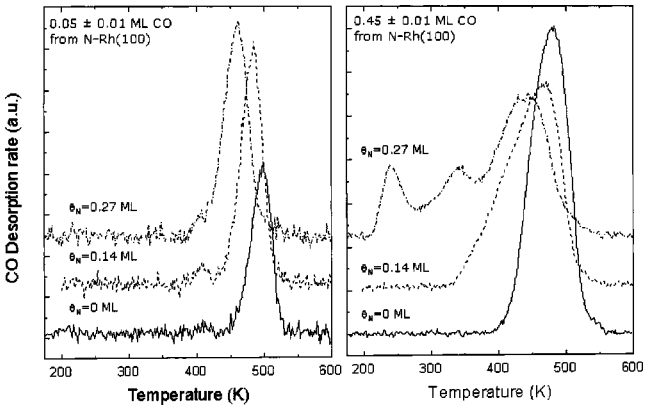

FIG. 6. Selected CO desorption rates from Figs. 1 and 3 for low (left panel) and high (right panel) CO coverages (not to scale with respect to each other) at two different N coverages.

oms and compressed CO. At the higher N coverage, new desorption features due to direct repulsion between CO and N are observed.

C. Quantification of the CO–N interaction

The results described above allow for an estimate of the CO–N repulsion between nearest neighbors. We associate the sharp 240 K CO desorption state in the TPD of CO from a $c(2\times2)$-N overlayer (Fig. 4) with the structural model presented in Fig. 4, with N atoms forming a $c(2\times2)$ structure adsorbed in four-fold hollow sites and CO molecules randomly placed in between. Theory predicts that atomic adsorbates such as N_{ads} are exclusively chemisorbed in the highest coordination site.[35] This is evidenced both by high-resolution EELS (HREELS) (Ref. 36) and DFT calculations (Ref. 37). As nitrogen atoms are much more strongly bound on Rh(100) than CO molecules, we assume that the preference of N_{ads} for the fourfold bonding site is not changed by the presence of coadsorbed CO_{ads}. The LEED data in Fig. 3 are in agreement with this assumption (albeit they do not form conclusive proof). We have also assumed that the Rh(100) substrate does not reconstruct upon coadsorption of N and CO. Although square-lattice (100)surfaces of different transition metals have been observed to reconstruct upon adsorption of atomic adsorbates, e.g., with O_{ads} on Rh(100) (Ref. 38) and N_{ads} on Ni(100) (Ref. 39), recent DFT calculations by Alfè *et al.*[40] predict that Rh(100) does not reconstruct upon adsorption of atomic N. Hence, we have tentatively placed the CO molecules in four-fold hollow sites in between four N atoms in neighboring positions. In order to compare the heat of adsorption of CO in the fourfold site in the presence of N atoms with CO on the otherwise empty Rh(100) surface, where it adsorbs in the on-top mode, we rely on the DFT calculations in Table II. The conclusion from these DFT calculations is that the heat of adsorption for CO does not vary appreciably between on-top, bridge, and hollow sites. Hence we assume that the experimentally determined value of 135 ± 5 kJ/mol also applies to CO if it were adsorbed in a fourfold site.

Now the pairwise repulsive interaction between CO_{ads} and N_{ads} (ω^{NN}_{CO-N}) can be derived from Eq. (1) by taking the difference in E_a between CO desorbing from Rh(100) and from $c(2\times2)$-N/Rh(100), divided by 4, because CO feels the repulsion from four neighboring N atoms. This yields $\omega^{NN}_{CO-N}\approx(E_{a,0}-E_{a,c(2\times2)})/4=19\pm3$ kJ/mol. Calculations by Curulla *et al.*[41] show an interaction of 30 kJ/mol. So the theoretical and experimental methods are in reasonable agreement.

Repulsion between CO_{ads} and N_{ads} is larger than repulsion between mutual CO molecules [$\omega^{NN}_{CO-N}=19$ kJ/mol versus $\omega^{NN}_{CO-CO}=9$ kJ/mol (Ref. 16)]. Together with the high mobility of CO,[27] this has important consequences for the lateral distribution of both adsorbates when coadsorbed. At low coverage, the first CO molecules are adsorbed on empty Rh patches where the heat of adsorption is only slightly decreased by small modification of the electrostatic potential. Increasing θ_{CO} leads to formation of separated domains of N_{ads} and compressed domains of CO, as the mutual repulsion between CO molecules is relatively small. Only when the surface becomes saturated in CO will additional CO molecules become adsorbed in between or close to N atoms, leading to increased repulsion between CO and N. This point of view is consistent with the observed changes in the CO desorption rate from Rh(100) and N-covered Rh(100).

D. Dynamic Monte Carlos simulations

In order to see to what extent the determined pairwise repulsion energy between CO and N on Rh(100) correctly predicts the experimental TPD data, we have carried out dynamic Monte Carlo simulations; see Fig. 7. Both CO and N were placed in a square grid of adsorption sites representing the Rh(100) substrate. Arrhenius rate parameters were taken from the TPD experiments, and mutual repulsion between CO molecules was ignored. Diffusion of neither CO nor N is allowed.

CO without N atoms (Fig. 7, top traces) is predicted to desorb around 500 K, in good agreement with the experiment (Fig. 1). The small shift of the maximum CO desorption rate to lower temperatures observed in the TPD experiments for low coverages ($\theta_{CO}<0.25$ ML) is probably due to repulsion between CO molecules in combination with their high mobility and is thus not reproduced in the simulations.

In the second set of simulations in Fig. 7 CO was adsorbed on a perfectly ordered $c(2\times2)$-N/Rh(100) surface, as depicted in the inset. For ω^{NN}_{CO-N} we have used the value of 19 kJ/mol, as derived from TPD experiments. Now the simulated CO desorption spectra are shifted to 230 K. This is in very good agreement with the peak temperature of the well-defined desorption state observed in TPD (Fig. 4) around 240 K, especially if we keep in mind the fact that we have not used any fitting parameter in the simulations. Also note that the simulated CO desorption spectra from the $c(2\times2)$-N/Rh(100) surface are sharper than those from Rh(100), in agreement with experiment.

The ill-defined desorption states in Fig. 4 at higher temperatures are probably due to desorption of CO from different adsorption sites, where CO has fewer neighboring N atoms due to defects in the $c(2\times2)$ nitrogen adlayer. Figure 8 shows different TPD spectra in which these defects are in-

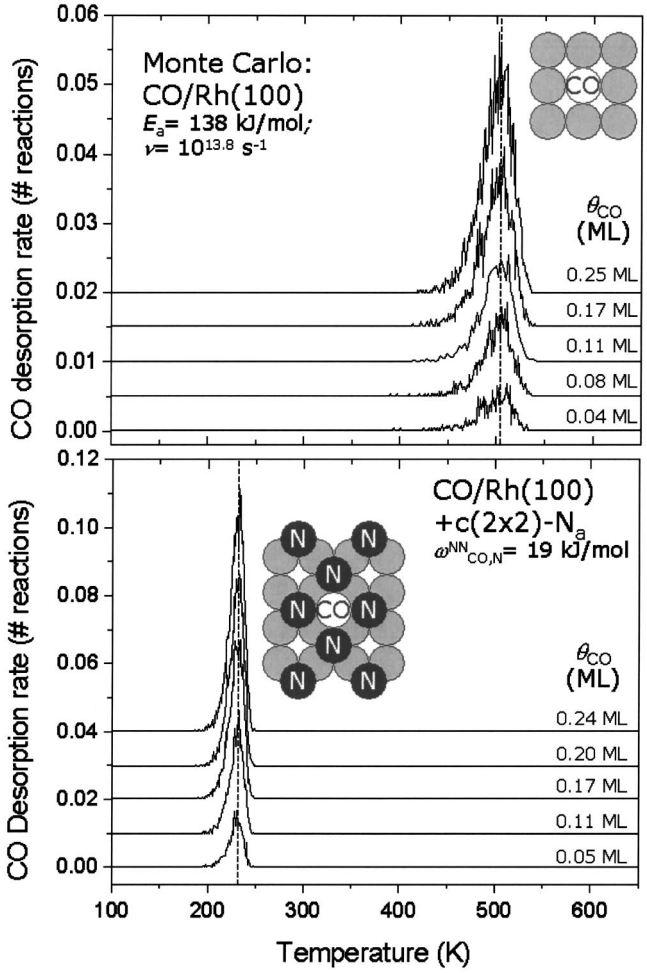

FIG. 7. Simulated CO desorption rates from Rh(100) (upper panel) and $c(2\times2)$-N/Rh(100) (lower panel) on a square 128×128 grid of sites using a dynamic Monte Carlo method. Kinetic parameters for CO desorption and pairwise lateral repulsive interaction between CO_{ads} and N_{ads} were taken from TPD experiments. The simulated heating rate was 5 K/s.

corporated in the Monte Carlo simulations. The peak around 300 K can be assigned to CO molecules, desorbing from a site with three neighboring N atoms. The feature around 370 K arises from CO molecules with two nitrogen neighbors. In the experiment the equivalent peak is not as strong, but here the peaks are much more smeared out over a broad temperature range, probably due to fast diffusion of CO on the defect $c(2\times2)$-N overlayer, thereby rapidly changing configurations. By including also a next-nearest-neighbor interaction, the peak around 415 K can also be reproduced. However, the value of ω^{NNN}_{CO-N} was fitted to 5 kJ/mol.

We conclude that the determined nearest-neighbor repulsion between CO and N atoms of 19 kJ/mol in combination with the assumption of pairwise additive interaction energies ($\Sigma_i n_i \omega_i^{NN}$) provides a quite accurate description of all features in the experimental TPD spectra of the CO–N coadsorbate system in Fig. 4. Defects in the $c(2\times2)$-N adlayer explain the additional desorption states.

V. CONCLUSIONS

Inclusion of lateral interactions on a square surface satisfactorily describes increased repulsion at high coverage, leading to destabilization of adsorbates, for example, in the desorption of CO from N-precovered Rh(100). This phenomenon is successfully simulated by a dynamic Monte Carlo (DMC) method. Using only experimentally determined parameters, the DMC method correctly reproduces the most important desorption features of the CO+N coadsorbate system on Rh(100).

It appears that in the adsorption of CO on Rh(100) a mobile precursor state is involved. The activation energy for desorption E_a at low coverages is 137 ± 2 kJ/mol and the preexponential factor ν is $10^{13.8\pm0.2}$ s^{-1}. The large discrepancy between the experimentally and theoretically determined adsorption energy (of 178 kJ/mol) and site for CO on Rh(100) calls for further theoretical investigation.

Coadsorbed N_{ads} destabilizes CO and lowers the CO saturation coverage. In the limit of zero CO coverage, E_a decreases with increasing θ_N, indicative for a lower heat of adsorption. This long-range effect is probably due to electronic modification of the Rh(100) surface by electronegative N atoms, suppressing backdonation from the metal d bands into the CO $2\pi^*$ state.

At higher CO coverage, additional desorption features appear in CO-TPD which are connected to short-range repulsive lateral interaction between CO_{ads} and N_{ads}. For CO de-

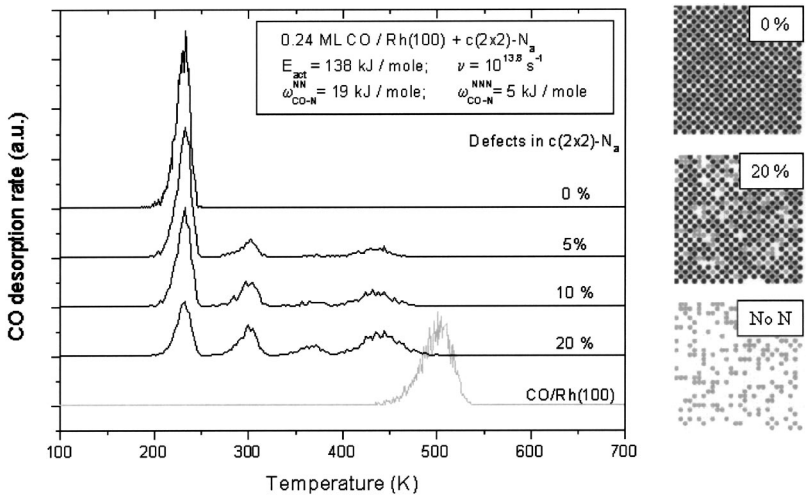

FIG. 8. Monte Carlo simulations of CO desorption coadsorbed with $c(2\times2)$-N overlayer containing defects. The next-nearest-neighbor interaction between CO and N has been optimized to fit the spectra of Fig. 4. The nearest-neighbor interaction and the kinetic parameters for desorption of CO from a clean Rh(100) surface have been determined in this work.

sorbing from a mainly ordered $c(2\times2)$-N structure we find $E_a=60$ kJ/mol. Considering the local environment of the desorbing CO molecules we derive $\omega_{\mathrm{CO-N}}^{\mathrm{NN}}=19$ kJ/mol. This value, along with the assumptions of pair-wise additive lateral interactions, gives a satisfactory description of the desorption of CO from CO+N coadsorption on Rh(100).

ACKNOWLEDGMENTS

This work was financially supported by the Netherlands Organization for Scientific Research–Chemical Sciences (NWO–CW) and performed under the auspices of the Netherlands Institute of Catalysis Research (NIOK).

[1] Y. Y. Yeo, L. Vattuone, and D. A. King, J. Chem. Phys. **104**, 8096 (1996).
[2] M. J. P. Hopstaken and J. W. Niemantsverdriet, J. Phys. Chem. B **104**, 3058 (2000).
[3] A. P. J. Jansen, Comput. Phys. Commun. **86**, 1 (1995).
[4] J. J. Lukkien, J. P. L. Segers, P. A. J. Hilbers, R. J. Gelten, and A. P. J. Jansen, Phys. Rev. E **58**, 2598 (1998).
[5] B. E. Nieuwenhuys, Adv. Catal. **44**, 259 (1999).
[6] V. P. Zhdanov and B. Kasemo, Surf. Sci. Rep. **19**, 31 (1997), and references herein.
[7] M. J. P. Hopstaken, W. J. H. van Gennip, and J. W. Niemantsverdriet, Surf. Sci. **433-435**, 69 (1999).
[8] M. J. P. Hopstaken and J. W. Niemantsverdriet, J. Chem. Phys. **113**, 5457 (2000).
[9] W. M. Daniel and J. M. White, Surf. Sci. **171**, 289 (1986).
[10] H. Höchst and E. Colavita, J. Vac. Sci. Technol. A **4**, 1442 (1986).
[11] G. A. Somorjai and E. L. Garfunkel, in *Physics and Chemistry of Alkali Metal Adsorption*, edited by H. P. Bonzel, A. M. Bradshaw, and G. Ertl (Elsevier, Amsterdam, 1989), p. 319.
[12] C. J. Zhang, P. Hu, and M.-H. Lee, Surf. Sci. **432**, 305 (1999).
[13] G. Klivényi and F. Solymosi, Surf. Sci. **420**, 17 (1999).
[14] A. M. de Jong and J. W. Niemantsverdriet, J. Phys. Chem. **101**, 10 126 (1994).
[15] P. Kisliuk, J. Phys. Chem. Solids **3**, 95 (1957).
[16] R. Kose, W. A. Brown, and D. A. King, J. Phys. Chem. B **103**, 8722 (1999).
[17] V. K. Medvedev, V. S. Kulik, V. I. Chernyi, and Y. Suchorski, Vacuum **48**, 341 (1997).
[18] B. A. Gurney, J. Lee, J. S. Villarubia, and W. Ho, J. Chem. Phys. **87**, 6710 (1987).
[19] F. Strisland, A. Ramstad, T. Ramsvik, and A. Borg, Surf. Sci. **415**, L1020 (1998).
[20] A. Baraldi, L. Gregoratti, G. Comelli, V. R. Dhanak, M. Kiskinova, and R. Rosei, Appl. Surf. Sci. **99**, 1 (1996).
[21] C.-M. Chan, R. Aris, and W. H. Weinberg, Appl. Surf. Sci. **1**, 360 (1978).
[22] P. A. Redhead, Vacuum **12**, 203 (1962).
[23] J. Kiss and F. Solymosi, Surf. Sci. **135**, 243 (1983).
[24] J. Kiss and F. Solymosi, J. Catal. **179**, 277 (1998).
[25] K. L. Kostov, H. Rauscher, and D. Menzel, Surf. Sci. **287/288**, 283 (1993).
[26] K. L. Kostov, P. Jacob, H. Rauscher, and D. Menzel, J. Phys. Chem. **95**, 7785 (1991).
[27] R. M. van Hardeveld, M. J. P. Hopstaken, J. J. Lukkien, P. A. J. Hilbers, A. P. J. Jansen, R. A. van Santen, and J. W. Niemantsverdriet, Chem. Phys. Lett. **302**, 98 (1999).
[28] K. Tanaka, T. Yamada, and B. E. Nieuwenhuys, Surf. Sci. **242**, 503 (1991).
[29] L. Casalis, A. Baraldi, G. Comelli, V. R. Dhanak, M. Kiskinova, and R. Rosei, Surf. Sci. **306**, 193 (1994).
[30] Y. Kim, H. C. Peebles, and J. M. White, Surf. Sci. **114**, 363 (1982).
[31] D. H. Wei, D. C. Skelton, and S. D. Kevan, Surf. Sci. **381**, 49 (1997).
[32] A. Eichler and J. Hafner, J. Chem. Phys. **109**, 5585 (1998).
[33] B. Hammer, L. B. Hansen, and J. K. Nørskov, Phys. Rev. B **59**, 7413 (1999).
[34] T. V. W. Janssens, G. R. Castro, K. Wandelt, and J. W. Niemantsverdriet, Phys. Rev. B **49**, 14599 (1994).
[35] R. A. van Santen and J. W. Niemantsverdriet, *Chemical Kinetics and Catalysis* (Plenum Press, New York, 1995).
[36] L. H. Dubois, J. Chem. Phys. **77**, 5228 (1982).
[37] D. Loffreda, D. Simon, and P. Sautet, J. Chem. Phys. **108**, 6447 (1998).
[38] J. R. Mercer, P. Finetti, F. M. Leibsle, R. McGrath, V. R. Dhanak, A. Baraldi, K. C. Prince, and R. Rosei, Surf. Sci. **352–354**, 173 (1996).
[39] E. Dudzik, A. G. Norris, R. McGrath, G. Charlton, G. Thornton, B. Murphy, T. S. Turner, and D. Norman, Surf. Sci. **433–435**, 317 (1999).
[40] D. Alfè, S. de Gironcoli, and S. Baroni, Surf. Sci. **437**, 18 (1999).
[41] D. Curulla, A. P. van Bavel, D. L. S. Nieskens, and J. W. Niemantsverdriet (unpublished).